New Role for Nonlinear Dynamics and Chaos in Integrated Semiconductor Laser Technology

M. Yousefi, Y. Barbarin, S. Beri, E. A. J. M. Bente, M. K. Smit, R. Nötzel, and D. Lenstra*

COBRA Research Institute, Technische Universiteit Eindhoven, The Netherlands

(Received 1 August 2006; published 23 January 2007)

Using an integrated colliding-pulse mode-locked semiconductor laser, we demonstrate the existence of nonlinear dynamics and chaos in photonic integrated circuits (PICs) by demonstrating a period-doubling transition into chaos. Unlike their stand-alone counterparts, the dynamics of PICs are more stable over the lifetime of the system, reproducible from batch to batch and on faster time scales due to the small sizes of PICs.

DOI: 10.1103/PhysRevLett.98.044101 PACS numbers: 05.45.Tp, 42.55.Px, 42.65.Sf

Integrated photonic devices containing large numbers of lasers will become increasingly important. Photonic flip-flops, as recently reported by some of us [1], allow for integration densities up to 10^5 components per cm^2. This will impose severe requirements on reproducibility of the circuits, similar to those reported for semiconductor devices in Ref. [2]. In integrated lasers, problems with reproduction may show up as unexpected dynamics of the output field, quite often referred to as unstable behavior or just noise [3,4]. However, it is the aim of this Letter to demonstrate that the output dynamics of the integrated optical devices which we have experimentally investigated are well behaving, well understandable, and well classifiable in terms of nonlinear dynamics. Systematic study of these dynamics provides fundamental insight into the underlying physics (a ''fingerprint'') of the integrated optical circuit, on the basis of which one can redesign the device and/or improve the processing, or simply exploit the dynamical performance of a particular device to one's advantage.

The semiconductor laser is known to be sensitive to perturbations and can easily show nonlinear dynamics in its performance due to a combination of strong phase-amplitude coupling, relatively high gain per length unit, and relatively long carrier recombination lifetime compared to the round-trip time of the cavity [5]. The most famous dynamical consequence of these factors is the relaxation oscillation, a damped periodic exchange between the intensity and inversion of the laser [6,7]. The resulting nonlinear dynamics are undesired features for many applications since they hamper the (cw and modulation) performance of the laser. So far, this has received not much attention from the technical community, with one notable exception, i.e., the work by Lippi *et al.* on enhancement of the modulation bandwidth by phase-space steering [8–10]. Current (binary) optical telecommunications technologies are focused on the mitigation of the nonlinear dynamics and the enhancement of ''stable'' behavior.

The last three decades of research on semiconductor laser dynamics has revealed that many dynamical states are actually stable modes of operation, of which continuous wave (cw) operation is a subset (see Ref. [6–8] and references therein). It is known that the dynamics arise due to the interplay of different time scales. It is known that the dynamics arise due to the interplay and research into phenomena as low frequency fluctuations (LFF) in semiconductor lasers with external feedback and the study of the dynamics of semiconductor lasers with optical injection [7] has helped to mature this scientific field so much that applications can now be made [8,10,12].

To mitigate and control dynamics, lower the costs, and increase the functionality as well as efficiency of optical components, integration of multiple optical components on a single chip is being pursued [13]. The decrease in size does indeed bring about many advantages, but the proximity of components on a photonic integrated circuit (PIC) makes it possible for components to couple much stronger and in novel configurations than a nonintegrated realization. As far as the dynamics are concerned, the small size tends to decrease the amount of possible operating modes, whereas the strong coupling creates new modes of operation such that the dynamical complexity remains present in a large parameter range for PICs. State-of-the-art material and processing technology is at a point where couplings can be reduced to a level as low as -50 dB between interfaces of different materials and components on a planar IC. Still, these small reflections are sufficient to induce non-cw dynamics [11]. A crucial step towards applications of nonlinear dynamics is the availability of a technique for experimental analysis and visualization of the dynamics, together with a rigorous theoretical description of the system, where each configuration on a PIC would require its own modeling. The aim of this Letter is to report on such analysis and visualization experiments realized in our laboratory. The results obtained clearly show a well-defined sequence of dynamics as a function of the pump current of the device: a so-called period-doubling route into chaos.

The device chosen for study is part of a series of colliding-pulse mode-locked lasers (CPMLL) [14] that were designed and fabricated for 40 GHz colliding-pulse passively mode-locked laser operation at an emission wavelength of 1.52 μm. Each chip consists of a 2 μm-wide active ridge waveguide semiconductor optical

amplifier (SOA) terminated by cleaved facets ($R = 0.35$) at the two ends (see inset Fig. 1). The small region in the center is electrically isolated and can be contacted independently. By reverse biasing this section a saturable absorber can be achieved. Such a configuration, consisting of a long amplifier section with a short absorber in the center, is designed to produce a train of picosecond optical pulses, but in practice the intended dynamics are hard to achieve. Instead, a variety of other dynamics may be observed, depending on the precise settings of the external control parameters, in this case the bias current and the absorber voltage [3,4].

The measurement setup is depicted in Fig. 1 together with a picture of an array of five CPMLLs. The chip was glued on a temperature controlled copper mount and the current and voltage were provided through two probes. Light from the laser output waveguides was collected using a lensed fibre. The signal was amplified using a SOA between two optical isolators in order to avoid feedback into the laser. The light was analyzed using a 50 GHz bandwidth photodiode connected to a 50 GHz electrical spectrum analyzer [Agilent E4448A], and a 1.25 GHz photodiode connected to a 4-gigasample/s oscilloscope with 1 GHz bandwidth and 2 megasamples per channel memory [LeCroy LT584-L]. The measured rf spectrum of the device suggests operation on many dynamical attractors as a function of the operation parameters (see, for instance, Fig. 3, right column). We observed strong dynamics in the frequency range up to 1 GHz at a reverse bias voltage of -2.4 V on the absorber. We fixed the absorber

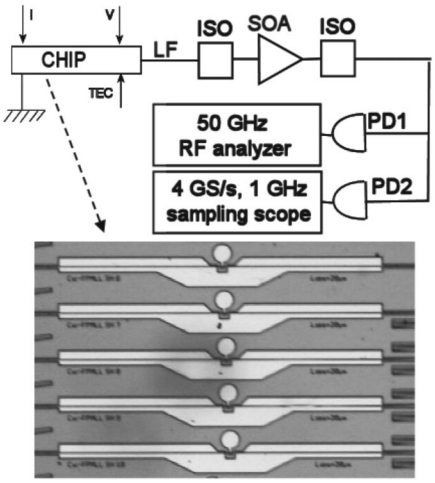

FIG. 1. The measurement setup with a picture of an array of five 40 GHz CPMLLs. The 40 μm-long absorber is shifted gradually from the center guaranteeing at least one laser with a perfectly cantered saturable absorber for mode locking. The results presented here are from the most asymmetric device (absorber 40 μm off from the center, lowest in the array). In the setup: I and V are the current and voltage sources, respectively, TEC is the temperature controller, ISO denotes the optical isolator, LF is the lensed fibre, and PD1 (50 GHz) and PD2 (1.25 GHz) are the two photo diodes.

voltage at this value and used the pump current of the SOA sections as the bifurcation parameter. From a bifurcation-theoretical point of view, in order to draw conclusions on characteristic routes to certain dynamics [7,15], it is very important that a sequence of transitions in dynamical behavior is observed as a function of a single parameter. We recorded the rf spectrum of the laser together with a 500 μs long time series (2×10^6 samples) of the output power and performed a statistical analysis on the data to reconstruct the deterministic content of the laser output dynamics.

For the statistical analysis, we first constructed a three-dimensional phase space $\mathbf{\Sigma}$ for the dynamics. We lay the time advanced power $P_\tau \equiv P(t + \tau)$ along one of the axes that span $\mathbf{\Sigma}$ and the power $P \equiv P(t)$ along the second. The choice of the delay time τ must follow some rationale: first, τ must be larger than the sampling time δt; second, τ should maximize the so-called fill factor [16], i.e., it should yield well-separated trajectories in $\mathbf{\Sigma}$. Consider, for example, a phase-space trajectory consisting of harmonic motion with period T. A choice $\tau = T/4$ leads to a circle in $\mathbf{\Sigma}$, while for $\tau = T/2$ (and integer multiples of T) the trajectory degenerates to a line, making the reconstruction impossible. In this work, the delay is set to $\tau = 4\delta t$ throughout this analysis, where $\delta t = 250$ ps is the sampling period of our oscilloscope. Note that unlike the Takens embedding technique [16], we do not use the value of τ to search for the embedding dimension of the attractors. In contrast, we perform statistical analysis of the phase-space trajectory, which is more robust to noise. For the third axis of $\mathbf{\Sigma}$ we took the time derivative of the power, estimated as $Q(t) \equiv \frac{[P(t)-P(t-\epsilon)]}{\epsilon}$, where ϵ is chosen as 0.3 ps. This quantity is proportional to the inversion level of the laser [5,6], an important dynamical variable.

Thus our system is represented by a phase-space trajectory $\vec{X}(t) = (P(t), P_\tau(t), Q(t))$, whose time evolution is assumed to be given by $\dot{\vec{X}}(t) = \vec{D}(\vec{X}(t)) + \vec{\xi}(t)$, where $\vec{D}$ governs the deterministic evolution and $\vec{\xi}(t)$ is the stochastic contribution to the dynamics. We will reconstruct $\vec{D}(\mathbf{\Sigma})$ using experimental data. The Langevin noise term is modeled with an additive white noise. The choice of multiplicative noise would have been more realistic [17]. However, as the oscillations in the power are small compared to the average level, the use of an additive noise term does not affect the qualitative features of the dynamics nor the reconstruction of a bifurcation sequence. We will operate our lasers at least 25% above threshold, thereby further reducing the relative influence of noise in the output signal. Finally, we assumed that the phase-space trajectory is a smooth curve in $\mathbf{\Sigma}$, which will allow us to interpolate our data using high order polynomials so as to achieve accurate values of P_τ and also use the interpolated data to improve the statistics of the trajectory if not enough data points exist.

During its evolution, the phase-space trajectory $\vec{X}(t)$ builds a density distribution in the phase space $\mathbf{\Sigma}$. This

distribution is assumed to correspond to a stationary solution of the Fokker-Planck Eq. [18,19], stochastically equivalent to the evolution equation of $\dot{\vec{X}}(t)$ that is denoted above. Roughly speaking, for a periodic motion such distribution would resemble a "tube," centered around the integral curves of $\vec{D}(\mathbf{\Sigma})$. The width of the "tube" depends on the noise diffusion strength. Clearly, for weak diffusion, the "tube" will be very narrow and its width will increase with the noise intensity. Above a certain limit intensity, the "tube" will blur out and it will be impossible to distinguish different parts of the "deterministic" motion. This gives a visual idea of the noise intensity beyond which our reconstruction scheme breaks down. This analysis also reinforces the idea that the embedding parameters must be chosen in order to maximize the fill factor. Parallel to the procedure outlined in Ref. [18], we calculate the average deterministic drift vector $\vec{D}$. Unlike Ref. [18], where the fundamental frequencies are on the order of kHz, we could not acquire a large amount of data points per period of oscillation since our fundamental frequencies were in the 1 GHz range. This is why we used polynomial interpolation and only focus on the deterministic content of the dynamics. Using the drift vector $\vec{D}$, we reconstruct the deterministic phase-space trajectory with a Euler-type spatial-integration method and recover the deterministic content of the phase-space trajectory of the CPMLL.

Figure 2 depicts one such result, where a subset of experimental data points is indicated in the phase space $\mathbf{\Sigma}$ by dots and the reconstructed deterministic phase-space trajectory by the solid green line. The projections of the phase portrait on the different phase planes are shown in black and red, respectively. It is clear from Fig. 2 that the phase space of our system is at least three-dimensional, since the period-4 limit cycle that the system exhibits is only visible in the 3D phase portrait (the self-intersection of the phase-space trajectory, visible in the two-dimensional phase plane projections, would be impossible for a real phase-space trajectory [15]). For the sake of clarity, in what follows we will restrict the visualization of the dynamics to projections on the phase planes $\sigma_1 \equiv (P, P_\tau)$ and $\sigma_2 \equiv (P, Q)$. However, in all cases the full 3D phase space has been used to calculate the drift vector and the deterministic phase-space trajectory.

Having established a methodology for the extraction and visualization of the deterministic dynamics exhibited by the device, we will now show how this method was used to study a series of bifurcations. Figure 3 depicts a sequence of dynamics as the pump current is varied from 133.5 mA to 139.5 mA with steps of 1 mA. The left column shows the phase portrait in the σ_1 plane and the middle column in the σ_2 plane. The last column shows the rf spectra of the output power up to 1 GHz. In the interval from 133.5 mA to 134.5 mA the laser is operating on a period-4 limit cycle with a fundamental period of 1.31 ns and a full period of 5.22 ns. When the current is increased to 135.5 mA, the limit cycle has lost its stability and the laser shows intermittent type of dynamics, which can be a precursor to chaos. Indeed, further increase of the pump current to 136.6 mA results in complex motion on a very long period, if not chaotic attractor, as can be concluded from both the rf spectra and the reconstructed deterministic trajectory. The chaotic dynamics are exited through a period-3 limit cycle, which appears when the current is further increased to 138.5 mA. The fundamental period of the limit cycle is $\sim$5 ns and a third of the period is $\sim$1.67 ns (600 MHz). At

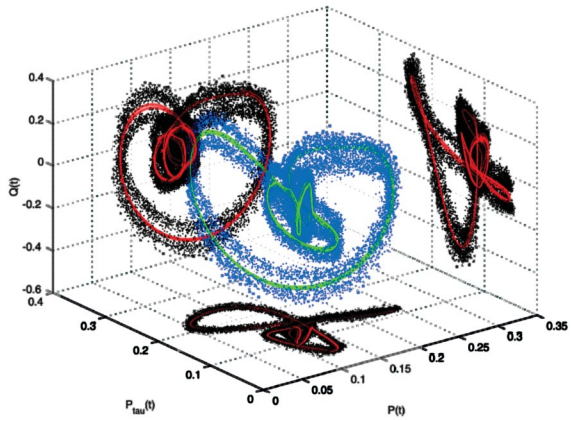

FIG. 2 (color). A portrait of the trajectory in $\mathbf{\Sigma}$. Blue dots indicate the sampled data points; solid green shows the reconstructed trajectory. Also the projections on the three phase planes have been shown, where black dots are the measured data points and the trajectory is indicated by a red solid line.

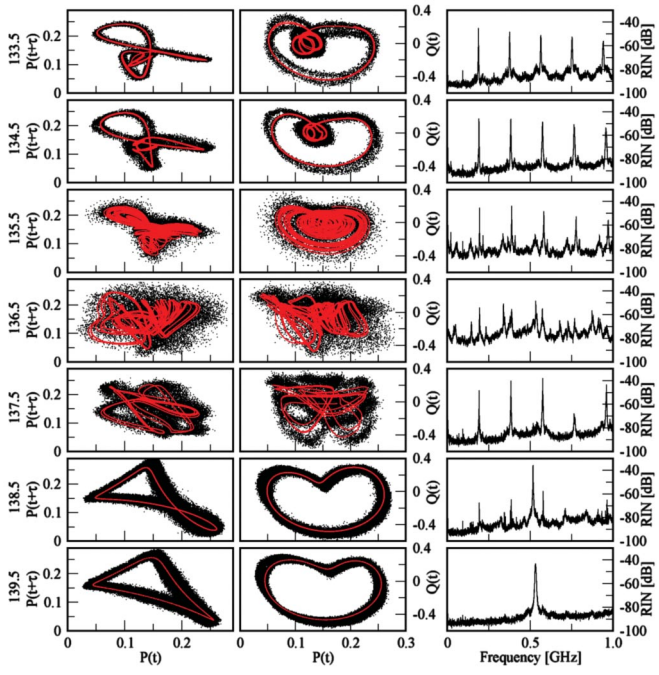

FIG. 3 (color). Phase plane portraits and rf spectra of the transition in and out of chaos of the CPMLL. The left column shows the phase portraits in σ_1, the middle column in σ_2, and the right column is the rf spectrum up to 1 GHz. The pump current is shown in the left corner of the plot in units of mili-Ampere.

138.5 mA, the laser shows single-period limit-cycle oscillations at a new frequency of 530 MHz while the corresponding spectrum shows a weak intermittency with the previous periodic dynamics. Note that the 530 MHz oscillations are probably related to the fast oscillations underlying the period-3 limit cycle at 138.5 mA. This period-1 limit cycle at 530 MHz stabilizes as the current is increased to 139.5 mA.

Although a special route of dynamics is presented here, we have observed many similar sequences in the ~1 GHz range in the output of the CPMLL's for various pump currents of the SOA and voltages and positions of the absorbers. Recently, a new batch of similar devices was processed, which lase at 1.55 μm and show similar nonlinear dynamical scenarios. Based on our observations, we conclude that integrated active photonic devices intrinsically show nonlinear dynamics. The physical explanation for one of the fundamental oscillation frequencies of the limit cycles in Fig. 3 is the beating between the two resonant frequencies of the compound cavity of the CPMLL. This beat frequency is a direct measure for the asymmetric positioning of the absorber region.

The current technological emphasis is on the narrowly defined so-called stable performance, which leads to a quest for stable performance of the optical devices and generally results in increased complexity of the device design and thus in higher costs. Our research reveals that integrated laser devices have no lesser tendency to show nonlinear dynamics than their nonintegrated counterparts composed of individual optical components. In fact, nonlinear dynamics occupy most of the parameter space of photonic integrated laser circuits (see, for instance, Ref. [3]) and their analysis and visualization can aid in their improved design.

By constructing a phase space and reconstructing the phase-space trajectory of the CPMLL, using a general Fokker-Planck type of analysis, we have demonstrated that the output of the CPMLL shows deterministic nonlinear dynamics. The method of Ref. [18] was improved by 6 orders of magnitude, in order to analyze dynamics on a GHz scale. Using experimental data alone, we reconstructed the drift vector $\vec{D}(\mathbf{\Sigma})$, which contains all relevant information of the deterministic part of the dynamics. The drift vector can be used to analyze the dynamics further and calculate other quantities such as Lyapunov exponents, the fractal dimension of attractors, etc. [15,17]. These quantities provide essential information for the exploitation of the PIC dynamics in applications such as chaotic encryption [12], phase-space steering [8–10], interferometric distance measurements, and broadband light sources. On the basis of the fingerprints of the CPMLL, it was even possible to identify the values of the control parameters to make the device operate as it was originally intended.

The current trend in photonics technology is towards large-scale photonic integration of components with complex functionalities, mainly consisting of networks of monolithically coupled devices. In this respect, the CPMLL analyzed here is not unique at all and confronts us with the fact that photonic integrated devices will inevitably exhibit deterministic nonlinear dynamics. The good news is that unlike their stand-alone counterparts, the dynamics of PICs are stable over the lifetime of the device and reproducible from batch to batch. These dynamics are well classifiable and well understood and ready to be exploited to our advantage.

The authors acknowledge the Towards Freeband Communication Impulse program of the Dutch Ministry of Economic Affairs within the NRC Photonics program. M. Y. is funded by the STW through the TWICE project.

*Also at LaserCentre, Vrije Universiteit, Amsterdam, The Netherlands.
Electronic address: m.yousefi@tue.nl

[1] M. T. Hill *et al.*, Nature (London) **432**, 206 (2004).
[2] T. Shinada, S. Okamoto, T. Kobayashi, and I. Ohdomari, Nature (London) **437**, 1128 (2005).
[3] T. Franck *et al.*, IEEE Photonics Technol. Lett. **8**, 40 (1996).
[4] L. A. Jiang, M. E. Grein, H. A. Haus, and E. P. Ippen, IEEE J. Sel. Top. Quantum Electron. **7**, 159 (2001).
[5] W. Chow, S. W. Koch, and M. Sargent III, *Semiconductor Laser Physics* (Springer-verlag, New York, NY, 1994).
[6] *Unlocking Dynamical Diversity: Optical Feedback Effects on Semiconductor Lasers*, edited by D. M. Kane and K. A. Shore (Wiley, New York, 2005).
[7] S. Wieczorek, B. Krauskopf, T. B. Simpson, and D. Lenstra, Phys. Rep. **416**, 1 (2005).
[8] G. L. Lippi *et al.*, J. Opt. B **2**, 375 (2000).
[9] B. Segard, S. Matton, and P. Glorieux, Phys. Rev. A **66**, 053819 (2002).
[10] N. Dokhane and G. L. Lippi, IEE Proceedings-Optoelectronics (1994-)/IEE Proc: Optoelectronics/IEE Proceedings-Optoelectronics **149**, 7 (2002).
[11] R. Tkach and A. Chraplyvy, IEEE J. of Lightwave Technology **4**, 1655 (1986).
[12] A. Argyris *et al.*, Nature (London) **438**, 04 275 (2005).
[13] See IEEE J. Sel. Top. Quantum Electron. (IEEE, New York, 2002), Vol. 6.
[14] Y. Barbarin *et al.*, *Proceedings of the ECOC 2005, Glasgow, Scotland* (ECOC, Glasgow, 2005), Vol. 3, We4.P.086, 673.
[15] E. Ott, *Chaos in Dynamical Systems* (Cambridge University Press, Cambridge, England, 1993).
[16] Th. Buzug and G. Pfister, Physica (Amsterdam) **58D**, 127 (1992).
[17] K. Petermann, *Laser Diode Modulation and Noise* (Springer-Verlag, Berlin, 1991).
[18] J. Gradišek, S. Siegert, R. Friedrich, and I. Grabec, Phys. Rev. E **62**, 3146 (2000).
[19] H. Risken, *The Fokker-Planck Equation* (Springer, New York, 1996), 2nd ed.